Scientia Iranica D (2019) 26(6), 3646–3655

SCIENTIA IRANICA

Sharif University of Technology

Scientia Iranica

Transactions D: Computer Science & Engineering and Electrical Engineering

http://scientiairanica.sharif.edu

Invited Paper

Incorporating bus-bar switching actions into AC optimal power flow to ovoid over-current status

M.A. Tavakkoli and N. Amjady*

Department of Electrical and Computer Engineering, Semnan University, Semnan, P.O. Box 35195-363, Iran.

Received 3 August 2019; received in revised form 18 September 2019; accepted 12 October 2019

KEYWORDS

Bus-bar switching actions;
Load shedding;
Over-Current (OC) relay;
Sub-transmission AC OPF;
Surge current.

Abstract. This paper presents a new AC Optimal Power Flow (AC OPF) model for sub-transmission networks. This model, which consists of sub-transmission and distribution bus-bar switching actions, can avoid undesirable Over-Current (OC) status and the subsequent actions of OC relays. The proposed AC OPF optimizes the bus-bar switching actions along with optimizing sub-transmission control actions. Also, to consider the impact of the actions of OC relays in the proposed AC OPF, the cost of load shedding caused by these relay actions is included in the objective function and minimized along with the sub-transmission operation cost. The bus-bar switching actions were modeled using binary decision variables. Therefore, the proposed AC OPF model is formulated as a Mixed-Integer Non-Linear Programming (MINLP) optimization problem. The effectiveness of the proposed model is illustrated for a real-world sub-transmission network of Iran's power system.

1. Introduction

Optimal Power Flow (OPF) optimizes the operating conditions of a power system by determining its optimal settings and control actions. Various OPF models, consisting of different objective functions, decision variables, and constraints, have been presented in the literature. A review of various OPF models and solution methods can be found in [1-3]. Recently, switching actions as an efficient way for power loss reduction [4,5], voltage profile improvement [6,7], and reliability enhancement [8,9] have been incorporated into the OPF problem. However, the focus of these OPF research works is on distribution network [4-7] or transmission network [8,9]. In the present research, we focus on sub-transmission network and its OPF operation function.

Sub-transmission network plays a crucial role in the electric power supply chain by acting as an intermediate network between transmission and distribution grids. While planning of sub-transmission network has been studied in some research works, such as [10-12], sub-transmission AC OPF is a more recent area of study [13,14]. Dehghanian and Kezunovic [13] investigated sub-transmission loss reduction through distribution network reconfiguration and in [14], a sub-transmission AC OPF based on load transferring between a pair of primary distribution feeders using distribution line switching maneuvers was presented. However, none of them studied optimizing switching actions of both sub-transmission and distribution grids in a coordinated manner.

A closed loop may be formed in sub-transmission and distribution networks in some switching maneuvers, leading to a large current in the switching period. If this current is higher than the OC relay setting, the OC relay action and unwanted load interruption occur. In [15-17], this current was evaluated as a surge current. In [17], in addition to calculating this surge current,

*. *Corresponding author. Tel.: +98 23 31532688*
E-mail addresses: mo-tavakoli@semnan.ac.ir (M.A. Tavakkoli); amjady@semnan.ac.ir (N. Amjady)

doi: 10.24200/sci.2019.54166.3625

superconducting fault current limiter was used to limit it. However, this solution adds considerable extra costs to the network. Also, none of the research works [15-17] studied OC relay action due to the surge current, nor they did model load interruption in an OPF framework. Thus, a sub-transmission OPF tool that can cope with these challenges is increasingly essential.

This research work proposes a new sub-transmission AC OPF model. This model optimizes both sub-transmission and distribution bus-bar switching actions, in addition to sub-transmission settings, to minimize sub-transmission operation cost and to avoid OC conditions caused by sub-transmission and distribution maneuvers. The following features discriminate the proposed AC OPF model from the previous works.

Previous OPF works including switching actions focus on a single network (e.g., distribution network or transmission network). However, the proposed AC OPF model includes bus-bar switching actions in both sub-transmission and distribution networks.

The proposed model optimizes sub-transmission and distribution switching maneuvers considering actions of the OC relays and the subsequent load sheds as well as power loss and cost of switching actions. Moreover, the proposed AC OPF model takes into account constraints of the OC relays of branches in addition to their thermal limits.

The proposed AC OPF model can limit the closed-loop surge currents by only changing the sub-transmission and distribution switching actions in a coordinated manner without adding fault current limiters and imposing their associated costs.

To better illustrate the new contributions of this research work, the uncertain parameters (e.g., load forecast uncertainty) are not considered in the proposed AC OPF model. However, they can be modeled in the proposed sub-transmission AC OPF approach using, e.g., scenario approach [18], stochastic programming [19], or robust optimization techniques [20,21].

The remainder of this paper is organized as follows. In Section 2, the proposed sub-transmission AC OPF model, including Sub-transmission and Distribution bus-bar switching actions to avoid undesirable OC statuses, is introduced. The numerical results obtained by the proposed sub-transmission AC OPF model for real-world Damavand sub-transmission network in Iran's power system are presented and discussed in Section 3. Section 4 concludes the paper.

2. Proposed sub-transmission AC OPF including sub-transmission and distribution bus-bar switching actions

In a sub-transmission network, dispatchers/operators continuously perform various switching maneuvers, e.g., for preventive maintenance purposes. However, during some of these sub-transmission maneuvers, unwanted OC statuses may occur, leading to the actions of OC relays and the subsequent load interruptions. Even in such situations, when OC relays do not operate properly or operate with delay, equipment damages (e.g., damage of secsioners) may be reported in practice. To avoid such unfavorable conditions, limiting these large surge currents by changing the switching maneuver using coordinated sub-transmission and distribution switching actions is proposed in this paper.

To better introduce this problem and the proposed solution method, an illustrative practical example is given in Figure 1. This figure shows a small portion of the real-world Damavand transmission/sub-transmission/distribution grid in Iran's power system. As can be seen, Buses 1 and 2 are the 230 kV and 400 kV buses, respectively, connected to other transmission substations. Buses 3 and 4 are in the secondary side of the 230 kV/63 kV and 400 kV/63 kV substations, respectively, to which Buses 5 and 6 are connected through 63 kV lines 1 and 2. Buses 7 and 8 are connected to the secondary side of the 63 kV/20 kV sub-transmission transformers. Buses 1-2, 3-6, and 7-8 are transmission, sub-transmission, and distribution buses, respectively. In Figure 1, SCB and DCB represent Sub-transmission and Distribution Circuit Breakers (CB), respectively. The status of each CB is specified by its color in Figure 1, where the black/white color shows that the corresponding CB is closed/open. SCB-1, SCB-2, SCB-3, and SCB-4 indicate line breakers in the sub-transmission grid, while SCB1 and DCB1 are bus-bar switches in the sub-transmission grid and the distribution grid, respectively. Usually, SCB1/DCB1 are normally closed/open CBs. In the sample network of Figure 1, the 63/20 kV sub-transmission substation is fed by 63 kV line 1 while 63 kV line 2 is considered to be the backup feeding path. Figure 1 shows a typical transmission/sub-transmission/distribution bus-bar configuration in the Iran's power system network.

Under specific conditions, e.g., preventive maintenance planning, it is necessary for the sub-transmission substation to be fed through line 2 rather than line 1. Therefore, it is required to close SCB-4 and then, open SCB-3. To do so, as shown in Figure 1, a ring is created in the short time period of the switching maneuver when both SCB-3 and SCB-4 are closed, which may yield a large surge current. The magnitude of this surge current depends on the 63 kV line impedances as well as the difference between the voltage phase angles of bus 3 and bus 4. This phase angle difference in turn depends on the loading conditions of the sub-transmission system. The produced large surge current may result in the action of the associated OC relays and the subsequent opening of SCB-1 and SCB-2. Thus, unwanted load shedding occurs in the sub-transmission

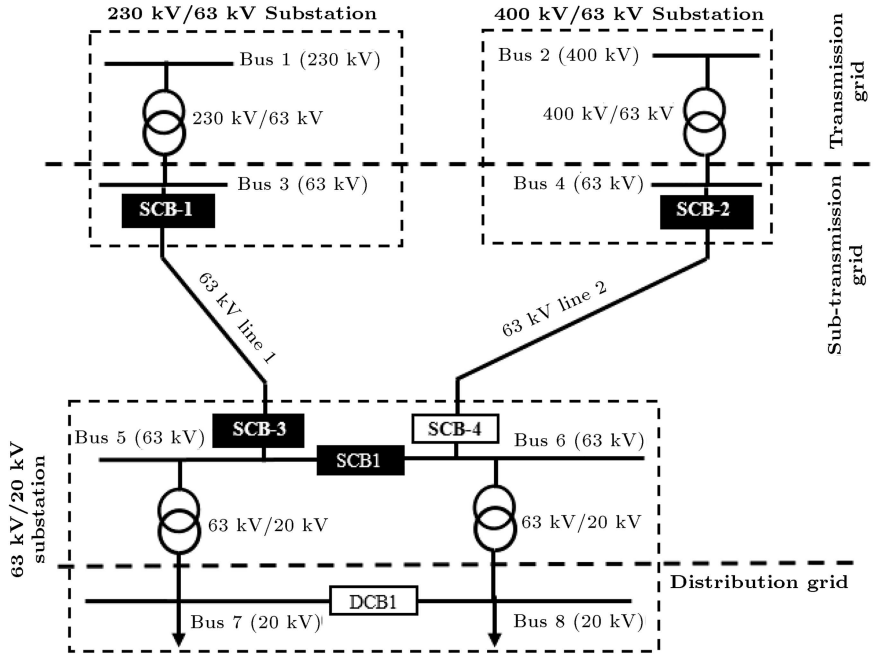

Figure 1. Two transmission substations and one sub-transmission substation in the real-world Damavand network in Iran.

system, leading to high operation costs. A typical solution to this problem is using fault current limiters [17], which impose significant additional costs on the sub-transmission system. The proposed sub-transmission AC OPF model can solve the problem of unwanted load shedding without requiring additional components.

In order to prevent this unwanted load curtailment, we propose to directly incorporate sub-transmission and distribution bus-bar switching actions (e.g., switching of SCB1 and DCB1 in the sample network of Figure 1) into the sub-transmission AC OPF problem. The output of this enhanced AC OPF problem will determine the status of the bus-bar switches, along with determining sub-transmission control actions, for a given operating point. In the case of closing DCB1 and opening SCB1, the current magnitude is limited as the impedances of the two 63/20 kV transformers are inserted in the current path. Thus, if the surge current value is higher than the specified setting of the OC relays, the OPF results in closing DCB1 and opening SCB1 to avoid the unwanted load interruption and its associated high cost. However, if the surge current magnitude is less than setting of the OC relays, the OPF results in retaining DCB1 open and SCB1 closed in order to reduce the number of switching actions as well as the network power loss.

Based on the concept outlined above, the proposed sub-transmission AC OPF model, incorporating sub-transmission and distribution bus-bar switching actions along with sub-transmission control actions, is formulated as:

$$\min_{P_i, Q_i, Pg_i, Ls_i, Qc_i, tc_{ij}, \phi_{ij}, Sw_{ij}} OF, \tag{1}$$

$$OF = \sum_{i \in \Omega_B} Cg_i \times Pg_i + \sum_{i \in \Omega_B} C^{LS} \times LS_i + \sum_{i \in \Psi_B} EP_i \times P_i + \sum_{ij \in \Omega_B} C^{PL} \times PL_{ij} + \sum_{ij \in \Omega_B} SC_{ij} \times n_{ij}^{sw}. \tag{2}$$

If tap/phase shifter setting is at bus i:

$$\begin{aligned} PL_{ij} =& Pb_{ij} + Pb_{ji} = \Big[(tc_{ij})^2 \times G_{ij} \times V_i^2 - V_i \\ & \times V_j \times tc_{ij} \times \Big(G_{ij} \cos(\delta_{ij} + \phi_{ij}) \\ & + B_{ij} \sin(\delta_{ij} + \phi_{ij})\Big)\Big] \\ & + \Big[G_{ij} \times V_j^2 - V_i \times V_j \times tc_{ij} \\ & \times \Big(G_{ij} \cos(\delta_{ji} - \phi_{ji}) + B_{ij} \sin(\delta_{ji} - \phi_{ji})\Big)\Big] \\ & \delta_{ij} = -\delta_{ji} \quad \text{and} \quad \phi_{ij} = \phi_{ji} \\ PL_{ij} =& G_{ij} \times \Big((tc_{ij})^2 \times V_i^2 + V_j^2 - 2 \times V_i \\ & \times V_j \times tc_{ij} \times \cos(\delta_{ij} + \phi_{ij})\Big). \end{aligned} \tag{3}$$

If tap/phase shifter setting is at bus j:

$$PL_{ij} = Pb_{ij} + Pb_{ji} = \Big[G_{ij} \times V_i^2 - V_i \times V_j \times tc_{ij} \times (G_{ij}\cos(\delta_{ij} - \phi_{ij}) + B_{ij}\sin(\delta_{ij} - \phi_{ij}))\Big] + \Big[(tc_{ij})^2 \times G_{ij} \times V_j^2 - V_i \times V_j \times tc_{ij} \times (G_{ij}\cos(\delta_{ji} + \phi_{ji}) + B_{ij}\sin(\delta_{ji} + \phi_{ji}))\Big]$$

$$\delta_{ij} = -\delta_{ji} \quad \text{and} \quad \phi_{ij} = \phi_{ji},$$

$$PL_{ij} = G_{ij} \times \Big(V_i^2 + (tc_{ij})^2 \times V_j^2 - 2 \times V_i \times V_j \times tc_{ij} \times \cos(\delta_{ij} - \phi_{ij})\Big), \tag{4}$$

$$P_i + Pg_i - Pd_i + LS_i = \sum_{j \in \Omega_B} Pb_{ij} \quad i \in \Psi_B, \tag{5}$$

$$Q_i + Pg_i \times tg(\cos^{-1}(PFg_i)) + Qc_i - (Pd_i - LS_i) \times tg(\cos^{-1}(PFd_i)) = \sum_{j \in \Omega_B} Qb_{ij} \quad i \in \Psi_B, \tag{6}$$

$$QPg_i - Pd_i + LS_i = \sum_{j \in \Omega_B} Pb_{ij} + \sum_{j \in (\Omega_B - \Psi_B)} P_{ij}^{Sw}, \quad i \in (\Omega_B - \Psi_B), \tag{7}$$

$$Pg_i - Pd_i + LS_i = \sum_{j \in \Omega_B} Pb_{ij} + \sum_{j \in (\Omega_B - \Psi_B)} P_{ij}^{Sw}, \quad i \in (\Omega_B - \Psi_B), \tag{8}$$

$$Pg_i \times tg(\cos^{-1}(PFg_i)) + Qc_i - (Pd_i - LS_i) \times tg(\cos^{-1}(PFd_i)) = \sum_{j \in \Omega_B} Qb_{ij} + \sum_{j \in (\Omega_B - \Psi_B)} Q_{ij}^{Sw}, \quad i \in (\Omega_B - \Psi_B). \tag{9}$$

If tap/phase shifter setting is at bus i:

$$Qb_{ij} = -(tc_{ij})^2 \times B_{ij} \times V_i^2 - V_i \times V_j \times tc_{ij} \times [G_{ij}\sin(\delta_{ij} + \phi_{ij}) - B_{ij}\cos(\delta_{ij} + \phi_{ij})], \quad i, j \in \Omega_B. \tag{10}$$

If tap/phase shifter setting is at bus j:

$$Pb_{ij} = G_{ij} \times V_i^2 - V_i \times V_j \times tc_{ij} \times [G_{ij}\cos(\delta_{ij} - \phi_{ij}) + B_{ij}\sin(\delta_{ij} - \phi_{ij})], \quad i, j \in \Omega_B. \tag{11}$$

If tap/phase shifter setting is at bus j:

$$Qb_{ij} = -B_{ij} \times V_i^2 - V_i \times V_j \times tc_{ij} \times [G_{ij}\sin(\delta_{ij} - \phi_{ij}) - B_{ij}\cos(\delta_{ij} - \phi_{ij})], \quad i, j \in \Omega_B, \tag{12}$$

$$(Pb_{ij})^2 + (Qb_{ij})^2 \le \left(Sb_{ij}^{\max}\right)^2, \quad i, j \in \Omega_B, \tag{13}$$

$$P_{ij}^{Sw} = Sw_{ij} \times \Big[Gsw_{ij} \times V_i^2 - V_i \times V_j \times (Gsw_{ij}\cos\delta_{ij} + Bsw_{ij}\sin\delta_{ij})\Big], \quad i, j \in (\Omega_B - \Psi_B), \tag{14}$$

$$Q_{ij}^{Sw} = Sw_{ij} \times \Big[Bsw_{ij} \times V_i^2 - V_i \times V_j \times (Gsw_{ij}\sin\delta_{ij} - Bsw_{ij}\cos\delta_{ij})\Big], \quad i, j \in (\Omega_B - \Psi_B), \tag{15}$$

$$\left(P_{ij}^{Sw}\right)^2 + \left(Q_{ij}^{Sw}\right)^2 \le \left(S_{ij}^{\max,Sw}\right)^2, \quad i, j \in (\Omega_B - \Psi_B), \tag{16}$$

$$V_i^{\min} \le V_i \le V_i^{\max}, \quad i \in \Omega_B, \tag{17}$$

$$Pg_i^{\min} \le Pg_i \le Pg_i^{\max}, \quad i \in \Omega_B, \tag{18}$$

$$Qg_i^{\min} \le Pg_i \times tg(\cos^{-1}(PFg_i)) \le Qg_i^{\max} \quad i \in \Omega_B, \tag{19}$$

$$(P_i)^2 + (Q_i)^2 \le (S_i^{\max})^2, \quad i \in \Psi_B, \tag{20}$$

$$Qc_i^{\min} \le Qc_i \le Qc_i^{\max}, \quad i \in \Omega_B, \tag{21}$$

$$0 \le LS_i \le Pd_i \quad i \in \Omega_B, \tag{22}$$

$$tc_{ij}^{\min} \leq tc_{ij} \leq tc_{ij}^{\max}, \quad i,j \in \Omega_B, \tag{23}$$

$$\phi_{ij}^{\min} \leq \phi_{ij} \leq \phi_{ij}^{\max}, \quad i,j \in \Omega_B, \tag{24}$$

$$Sw_{ij} \in \Omega_S \quad i,j \in (\Omega_B - \Psi_B). \tag{25}$$

If phase shifter/tap setting is at bus i, then Eq. (26) shown in Box I is obtained.

If phase shifter/tap setting is at bus j, then Eqs. (27) and (28) shown in Box II are obtained.

The decision variables of the proposed AC OPF model are indicated in Relation (1), including sub-transmission control actions (i.e., P_i, Q_i, Pg_i, LS_i, Qc_i, tc_{ij}, and ϕ_{ij}) and bus-bar switching actions (i.e., Sw_{ij}). Sub-transmission OPF functions, which are regularly run in sub-transmission dispatch centers, should minimize the operation cost of their sub-transmission systems. Thus, the objective function of the proposed sub-transmission AC OPF model includes DG generation cost, load shedding cost, purchased power cost, power loss cost, and switching cost as presented in the 5 summations of Eq. (2), respectively. The purchased power supplies both sub-transmission load demand and power loss. However, since power loss minimization is usually essential for sub-transmission system dispatchers/operators in practice, the power loss cost has also been included as a separate term in the Objective Function (OF) in Eq. (2). Except for the power loss cost, all the terms of the OF are directly proportional to one of the decision variables and thus, can be easily determined. However, the power loss cost is directly proportional to the power loss, which is a function of the decision variables. Thus, AC power loss as a function of the decision variables is formulated in Eqs. (3) and (4). Using $\delta_{ij} = -\delta_{ji}$ (based on its definition as phase angle difference) and $\phi_{ij} = \phi_{ji}$ (as its minus sign has been separately considered in the associated equations), the power loss function has been simplified in Eqs. (3) and (4).

Active and reactive power balance equations at the boundary buses Ψ_B of sub-transmission network, connected to upstream transmission grid, are given in Eqs. (5) and (6), respectively. Active and reactive power balance constraints on the remaining $\Omega_B - \Psi_B$ buses considering active/reactive power flows of bus-bar switches are presented in Eqs. (7) and (8), respectively. Active and reactive branch flows considering phase shifter/tap changing capability are given in Eqs. (9)-(12). For lines, phase shifter setting and tap setting are fixed to zero and one, respectively. Apparent power flows of branches are limited in Relation (13). Active and reactive power flows of switches are given in Eqs. (14) and (15). The apparent power flows of switches are limited in Relation (16). Limits on voltage magnitudes are shown in Relation (17). Relation (18) bounds the active power generated by DGs. Similarly, reactive power of DGs is constrained to their allowable ranges in Relation (19). The power purchased from upstream transmission grid is limited in terms of the apparent power capacities of boundary substations in Relation (20). The constraints on the reactive power of shunt compensators, load sheds, tap settings, and phase shifter settings are given in Relations (21), (22), (23), and (24), respectively. Feasible space of bus-bar switching actions is presented in Relation (25). For instance, for the illustrative example of Figure 1, Relation (25) includes:

$$\text{SCB1} + \text{DCB1} \geq 1, \tag{29}$$

to supply both distribution feeders. For the sake

$$I_{ij} = \left(\begin{array}{l} [tc_{ij} \times V_i \times (G_{ij} \times \cos(\delta_i + \phi_{ij}) - B_{ij} \times \sin(\delta_i + \phi_{ij})) - V_j \times (G_{ij} \times \cos(\delta_j) - B_{ij} \times \sin(\delta_j))]^2 \\ + [tc_{ij} \times V_i \times (G_{ij} \times \sin(\delta_i + \phi_{ij}) + B_{ij} \times \cos(\delta_i + \phi_{ij})) - V_j \times (G_{ij} \times \sin(\delta_j) + B_{ij} \times \cos(\delta_j))]^2 \end{array} \right)^{\frac{1}{2}}$$

$$i,j \in \Psi'_B. \tag{26}$$

Box I

$$I_{ij} = \left(\begin{array}{l} [V_i \times (G_{ij} \times \cos(\delta_i) - B_{ij} \times \sin(\delta_i)) - tc_{ij} \times V_j \times (G_{ij} \times \cos(\delta_j + \phi_{ij}) - B_{ij} \times \sin(\delta_j + \phi_{ij}))]^2 \\ + [V_i \times (G_{ij} \times \sin(\delta_i) + B_{ij} \times \cos(\delta_i)) - tc_{ij} \times V_j \times (G_{ij} \times \sin(\delta_j + \phi_{ij}) + B_{ij} \times \cos(\delta_j + \phi_{ij}))]^2 \end{array} \right)^{\frac{1}{2}}$$

$$i,j \in \Psi'_B \quad i,j \in \Psi'_B, \tag{27}$$

$$I_{ij} \leq I_{ij}^{oc}, \quad i,j \in \Psi'_B. \tag{28}$$

Box II

of brevity and better illustrating the proposed idea, each of the sub-transmission and distribution sides in the 63/20 kV substation in Figure 1 has only two bus sections and one bus-bar switch. However, the proposed AC OPF model can consider any number of bus sections and any number of bus-bar switches in which Relation (25) specifies feasible switching actions based on the substation configuration.

Branch currents are calculated in Eqs. (26) and (27), considering phase shifter/tap settings, and constrained in Relation (28) in terms of the limits on OC relays. Thus, the proposed AC OPF model manages sub-transmission and distribution bus-bar switching actions in a way that no OC relay limit violation, leading to unwanted load shedding, occurs. Another essential advantage of the proposed AC OPF approach is modeling and applying both thermal limits and the limits on OC relays of branches, which provides a more secure operating point for sub-transmission networks than the previous sub-transmission OPF approaches do.

3. Numerical results

The proposed AC OPF model has been tested on the real-world Damavand sub-transmission network in Iran's power system. This network includes 30 sub-transmission 63 kV/20 kV substations, 67 sub-transmission 63 kV/20 kV transformers, 57 sub-transmission 6 3kV lines, 2 DGs (with the capacities of 10 MW and 5.5 MW), and 25 shunt compensators. The active and reactive loads of the network snapshot considered for the AC OPF study are 882.6 MW and 335.5 MVAR, respectively. The proposed OPF model has been implemented within GAMS programming environment and solved using KNITRO solver [22]. In the simulation studies of this section, the required economic data were obtained from [23].

To evaluate the effectiveness of the proposed sub-transmission AC OPF model, its results are compared with the results of two other sub-transmission AC OPF models in Table 1. The decision variables, Sw_{ij}, in the AC OPF model 1 include only bus-bar switching actions at sub-transmission level, in the AC OPF model 2 include only bus-bar switching actions at distribution level, and in the AC OPF model 3 include both sub-transmission and distribution bus-bar switching actions. Since the AC OPF model 1 does not include bus-bar switching actions in distribution level, it cannot limit the surge current values. Thus, this AC OPF model has the formulations given in Eqs. (1)-(25), leaving out Eqs. (26)-(28), which are used to model and limit the surge current. However, the AC OPF models 2 and 3 in Table 1 have the complete formulations given in Eqs. (1)-(28) as they can limit the surge current values. The AC OPF models 1 and 2 in Table 1 are two comparative models, while the AC OPF model 3 is the proposed one. AC OPF model without switching actions has not been considered for comparison here. This is due to the fact that such AC OPF model may not be practical for sub-transmission networks where the dispatchers/operators frequently encounter switching maneuvers, e.g., for performing preventive maintenance or changing the supply paths.

As described in the previous section, the purchased power supplies both the sub-transmission load demand and power loss. Thus, the total cost reported in Table 1 includes the cost of purchased power, the cost of DG operation, the cost of load shedding, and the cost of switching reported in columns 2, 3, 4, and 5 of the table, respectively. The cost of power loss values is reported in the last column of Table 1, after the total cost, for comparing the power losses of the three AC OPF models. Since all the AC OPF models fully utilize the two DGs in the considered snapshot, the same DG operation cost has been reported for the three AC OPF models.

In the AC OPF model 1, some load sheds are observed due to the OC status occurring in some switching maneuvers and the subsequent actions of the associated OC relays. In the AC OPF model 2, unwanted load shedding does not occur. However, since impedances of the two 63/20 kV transformers are inserted in the current path of all bus-bar switching maneuvers, the amount of power loss increases in this model, which can be observed in the column devoted to the cost of power loss in Table 1. In addition, the AC OPF model 2 has a higher switching cost value than the AC OPF model 1, since it incurs more bus-bar switching actions. However, the total cost in the AC OPF model 2 is lower than that in the AC OPF model 1, because it does not incur the high cost of load shedding. The proposed AC OPF model 3 with a lower cost of power loss and a lower cost of switching than the AC OPF model 2 has the same important advantage of this model, i.e., it can eliminate the unwanted load

Table 1. Results obtained for real-world Damavand sub-transmission system.

OPF model	Cost of purchased power [$]	Cost of DG operation [$]	Cost of load shedding [$]	Cost of switching [$]	Total cost [$]	Cost of power loss [$]
1	32778	558	4277	60	37673	571
2	33030	558	0	450	34038	630
3	33022	558	0	190	33770	622

Table 2. Results obtained for real-world Damavand sub-transmission system with a higher loading level.

OPF model	Cost of purchased power [$]	Cost of DG operation [$]	Cost of load shedding [$]	Cost of switching [$]	Total cost [$]	Cost of power loss [$]
1	38754	558	18670	84	58066	714
2	39673	558	0	630	40861	793
3	39658	558	0	266	40482	779

shedding. This leads to the lower total cost of the proposed AC OPF model 3 than those of both the AC OPF models 1 and 2. The proposed AC OPF model selects the best switching mode (between sub-transmission bus-bar switching and distribution bus-bar switching) in each sub-transmission maneuver. In addition, the proposed AC OPF model optimizes sub-transmission and distribution bus-bar switching actions along with optimizing other sub-transmission control actions.

The results obtained by the three AC OPF models for Damavand sub-transmission network in another snapshot are reported in Table 2. The snapshot of Table 2 has about 20% higher loading level of the system than the snapshot of Table 1. It is worthwhile to mention that both the snapshots considered for the numerical experiments of Tables 1 and 2 include realistic data, which have been practically reported in the associated sub-transmission dispatch center. The columns of Table 2 are identical to those of Table 1. By comparing the results reported in Tables 1 and 2, the following points can be concluded:

1. The same DG operation costs as those in Table 1 have been obtained in Table 2, since the three AC OPF models fully utilize the DGs in the numerical experiment of Table 2, similar to the numerical experiment of Table 1;
2. The cost of load shedding of the AC OPF model 1 in Table 2 is significantly higher than that of this model in Table 1. The reason can be described as follows. The snapshot of Table 2 has a higher system loading level than the snapshot of Table 1. As described for the sample network of Figure 1, the magnitude of the switching surge current depends on the 63 kV line impedances as well as the difference between the voltage phase angles of bus 3 and bus 4. A higher loading level of the sub-transmission system increases this phase angle difference, which leads to a more serious surge current. The more serious surge currents result in more actions of OC relays and thus, further unwanted load interruptions are yielded. Accordingly, a higher value of load shedding cost is obtained for the AC OPF model 1 in Table 2. However, Table 2 shows that the AC OPF models 2 and 3 can still avoid the unwanted load shedding and its associated high cost;
3. The cost of power loss and the cost of switching of all the AC OPF models have higher values in Table 2 than in Table 1, due to the higher system loading level considered in the numerical experiment of Table 2. In addition, these tables show that the cost of power loss and the cost of switching have higher increases in the AC OPF models 2 and 3 than in the AC OPF model 1. The reason is that the AC OPF models 2 and 3 should limit a higher number of surge currents using bus-bar switching actions in the snapshot of Table 2;
4. In Table 2, it is seen that the total costs of the AC OPF models 2 and 3 are considerably lower than the total cost of the AC OPF model 1. This is due to the fact that, among the opposing cost components presented in the above points 2 and 3, the cost of load shedding has a significantly higher value than the cost of power loss and the cost of switching values;
5. Table 2 shows that the proposed AC OPF model 3 has a lower total cost value than the two comparative AC OPF models 1 and 2. In addition, high differences are seen between the total cost value of the proposed AC OPF model 3 and the total cost values of the AC OPF models 1 and 2 in Table 2 compared to Table 1. This indicates that the effective performance of the proposed AC OPF model to avoid unwanted load shedding and to minimize sub-transmission system operation cost is highlighted in heavier loading conditions;
6. Convexification methods (such as signomial convexification [24], second-order cone programming [25], and semi-definite relaxation [26]) and linearization methods (such as McCormick relaxation [27], piecewise linearization [28], and least square technique [29]) have recently been applied to the OPF problem to make it tractable. However, these methods are mostly suitable for OPF of transmission networks, which is typically a large optimization problem with many binary variables. However, the proposed OPF approach has been proposed for sub-transmission networks. Regarding these networks, the following points can be mentioned:
   a) Sub-transmission networks are usually local grids, which are smaller than transmission networks;
   b) The loops that are analyzed in the paper are formed in the transient period. However, in

the steady-state operation, sub-transmission networks are usually operated radially to decrease short circuit level. Thus, the number of their switching actions (which is the number of binary variables in the OPF optimization problem) is typically lower than the number of switching actions in transmission networks with meshed operation. Additionally, in the proposed OPF, we only focus on the switching actions that are used to change the supply path, further decreasing the number of binary variables.

The above points (a) and (b) indicate that the proposed sub-transmission OPF is a smaller optimization problem with a lower number of binary variables than transmission OPF problems. Thus, its computation burden is not as critical as the computation burden of transmission OPF problems. As a practical evidence in this regard, the test case of this paper (i.e., Damavand sub-transmission network) is one of the largest sub-transmission networks that has a sub-transmission dispatch center (and thus, sub-transmission OPF can be run for it) in Iran's power system. The execution time of the proposed sub-transmission OPF with MINLP model for this sub-transmission network is only about 5 min (measured on a 64-bit Windows-based server with 40 GB of RAM and 24 Intel Xeon processors clocking at 2.2 GHz), which is a reasonable computation time. In addition, convexification/linearization methods usually encounter convexification/linearization errors. To avoid these errors, we have used the exact MINLP model of the OPF problem in this paper as it is tractable for sub-transmission networks.

4. Conclusions

In this paper, a new AC OPF model for sub-transmission systems has been presented. In practice, sub-transmission system dispatchers/operators frequently perform switching maneuvers for various operation purposes, such as fulfilling preventive maintenance plans or modifying supply paths, based on the current loading conditions of the system. These switching maneuvers may lead to surge currents during the switching period. Such surge currents may not be tolerable for the sub-transmission system, leading to the actions of the OC relays and unwanted load shedding. The proposed AC OPF model could overcome the problem of switching surge currents without requiring additional components, while minimizing the operation cost of sub-transmission system. For this purpose, the proposed model incorporated sub-transmission and distribution bus-bar switching actions into the sub-transmission AC OPF problem.

By testing the proposed AC OPF model for a real-world sub-transmission system, it was shown that the proposed model could avoid the undesirable OC status and actions of OC relays in sub-transmission switching maneuvers with a minimum increase in the power loss and switching cost. In addition, it was illustrated that the effective performance of the proposed AC OPF model was highlighted in higher sub-transmission system loading levels.

Extending the proposed AC OPF model to: 1) include and optimize line switching actions along with bus-bar switching actions for a more effective operation of sub-transmission systems, and 2) consider and model uncertain parameters (such as load forecast uncertainty) of sub-transmission system are directions for future research works.

In addition, recently, analyzing joint sub-transmission and primary distribution networks has been demanded in sub-transmission dispatch centers as these networks are usually highly connected in practice. These joint networks are larger than sub-transmission grids. Moreover, the number of their binary variables is significantly higher than the number of binary variables in sub-transmission networks due to a large number of switches in primary distribution feeders. Thus, extending the proposed sub-transmission OPF to optimize the operating point of joint sub-transmission and primary distribution networks may require appropriate convexification/linearization methods. This can also be considered as the future research direction.

Nomenclature

Indices

i, j	Bus indices

Sets

Ψ_B	Set of sub-transmission boundary buses connected to transmission grid
$\Psi_{B'}$	Subset of Ψ_B including buses which can create a loop by sub-transmission/distribution bus-bar switching actions
Ω_B	Set of sub-transmission buses
Ω_S	Feasible space of bus-bar switching actions

Parameters

B_{ij}	Susceptance of branch $i-j$
G_{ij}	Conductance of branch $i-j$
Bsw_{ij}	Susceptance of bus-bar switch $i-j$
Gsw_{ij}	Conductance of bus-bar switch $i-j$
C_{gi}	Generation cost of DG located at bus i

C^{LS} Load shedding cost

C^{PL} Cost of active power loss

SC_{ij} Switching cost of bus-bar switch $i-j$

EP_i Energy purchase price at bus i

Pd_i Active power demand at bus i

$Pg_i^{\min}$ Minimum limit of Pg_i

$Pg_i^{\max}$ Maximum limit of Pg_i

PFd_i Power factor of load at bus i

PFg_i Power factor of DG at bus i

$Qc_i^{\min}$ Minimum limit of Qc_i

$Qc_i^{\max}$ Maximum limit of Qc_i

$Qg_i^{\min}$ Minimum limit of Qg_i

$Qg_i^{\max}$ Maximum limit of Qg_i

$S_i^{\max}$ Maximum apparent power capacity of sub-transmission boundary bus i

$S_{ij}^{\max,sw}$ Maximum apparent power flow limit of bus-bar switch $i-j$

$Sb_{ij}^{\max}$ Maximum apparent power flow limit of branch $i-j$

$tc_{ij}^{\min}$ Minimum limit of tc_{ij}

$tc_{ij}^{\max}$ Maximum limit of tc_{ij}

$V_i^{\min}$ Minimum limit of V_i

$V_i^{\max}$ Maximum limit of V_i

$\phi_{ij}^{\min}$ Minimum limit of ϕ_{ij}

$\phi_{ij}^{\max}$ Maximum limit of ϕ_{ij}

Variables

I_{ij} Current flow of branch $i-j$

I_{ij}^{OC} OC relay limit of branch $i-j$ in terms of I_{ij}

LS_i Load shedding of bus i

n_{ij}^{sw} Number of switching actions of bus-bar switch $i-j$

OF Objective function of sub-transmission AC OPF model

P_i Active power purchased from the upstream grid (i.e., transmission network) at bus i

Pb_{ij} Active power flow of branch $i-j$

Pg_i Active power generated by the DG located at bus i

PL_{ij} Active power loss of branch $i-j$

P_{ij}^{sw} Active power flow of bus-bar switch $i-j$

Q_i Reactive power received from the upstream grid (i.e., transmission network) at bus i

Qb_{ij} Reactive power flow of branch $i-j$

Qc_i Reactive power of capacitor located at bus i

Qg_i Reactive power generated by the DG located at bus i

Q_{ij}^{sw} Reactive power flow of bus-bar switch $i-j$

Sw_{ij} Binary variable indicating status of bus-bar switch $i-j$, where 1/0 represents closed/open status

tc_{ij} Tap setting of tap-changing transformer $i-j$

V_i Voltage magnitude of bus i

δ_i Voltage angle of bus i

δ_{ij} Phase angle difference between bus i and bus j

ϕ_{ij} Setting of phase shifter $i-j$

References

1. Capitanescu, F. "Critical review of recent advances and further developments needed in AC optimal power flow", *Electr. Power Syst. Res.*, **136**, pp. 57-68 (2016).
2. Abdi, H., Beigvand, S.D., and Scala, M.La. "A review of optimal power flow studies applied to smart grids and microgrids", *Renew. Sustain. Energy Rev.*, **71**, pp. 742-766 (2017).
3. Maskar, M.B., Thorat, A.R., and Korachgaon, I. "A review on optimal power flow problem and solution methodologies", *2017 Int. Conf. Data Manag. Anal. Innov. ICDMAI 2017*, pp. 64-70 (2017).
4. Pegado, R., Ñaupari, Z., Molina, Y., et al. "Radial distribution network reconfiguration for power losses reduction based on improved selective BPSO", *Electr. Power Syst. Res.*, **169**, pp. 206-213 (2019).
5. Murty, V.V.V.S.N. and Sharma, A.K. "Optimal coordinate control of OLTC, DG, D-STATCOM, and reconfiguration in distribution system for voltage control and loss minimization", *Int. Trans. Electr. Energy Syst.*, **29**(3), pp. 1-27 (2019).
6. Gholami, K., Karimi, S., and Dehnavi, E. "Optimal unified power quality conditioner placement and sizing in distribution systems considering network reconfiguration", *Int. J. Numer. Model. Electron. Networks, Devices Fields*, **32**(1), pp. 1-17 (2019).
7. Home-Ortiz, J.M., Vargas, R., Macedo, L.H., et al. "Joint reconfiguration of feeders and allocation of capacitor banks in radial distribution systems considering voltage-dependent models", *Int. J. Electr. Power Energy Syst.*, **107**, pp. 298-310 (2019).
8. Salkuti, S.R. "Congestion management using optimal transmission switching", *IEEE Syst. J.*, **12**(4), pp. 3555-3564 (2018).
9. Xiao, R., Xiang, Y., Wang, L., et al. "Power system reliability evaluation incorporating dynamic thermal

rating and network topology optimization", *IEEE Trans. Power Syst.*, **33**(6), pp. 6000-6012 (2018).

10. Jalali, M., Zare, K., and Hagh, M.T. "A multi-stage MINLP-based model for sub-transmission system expansion planning considering the placement of DG units", *Int. J. Electr. Power Energy Syst.*, **63**, pp. 8-16 (2014).
11. Rad, H.K. and Moravej, Z. "Sub-transmission sub-station expansion planning based on bacterial foraging optimization algorithm", *J. AI Data Min.*, **5**(1), pp. 11-20 (2017).
12. Abedi, M.H., Hosseini, H., and Jalilvand, A. "Sub-transmission substation expansion planning considering load center uncertainties of size and location", *Int. J. Electr. Power Energy Syst.*, **109**, pp. 413-422 (2019).
13. Dehghanian, P. and Kezunovic, M. "Impact assessment of transmission line switching on system reliability performance", *2015 18th Int. Conf. Intell. Syst. Appl. to Power Syst. ISAP 2015* (2015).
14. Tavakkoli, M.A. and Amjady, N. "A new AC OPF tool for sub-transmission networks considering distribution switching actions and load-transferring capability", *Int. Trans. Electr. Energy Syst.*, **29**(8), pp. 1-17 (2019).
15. Feng, J., Zhang, J.H., and Liu, R.X. "Analysis of surge current due to closing loop in distribution network", In *Proc. 8th Int. Conf. Adv. Power Syst. Control Oper. Manag.*, Hong Kong, China, pp. 1-5 (2009).
16. Yin, Q., Ding, R., Zhao, Y., et al. "The feasibility research on distribution network closed loop based on the load transfer model", *World J. Eng. Technol.*, **05**(04), pp. 12-20 (2017).
17. Li, Z., Chen, L., Yang, W., et al. "Using hybrid type SFCL to limit the surge current caused by closing loop operation in distribution system", *Appl. Mech. Mater.*, **556-562**, pp. 1647-1651 (2014).
18. Rahmani, S. and Amjady, N. "A new optimal power flow approach for wind energy integrated power systems", *Energy*, **134**, pp. 349-359 (2017).
19. Sharifzadeh, H., Amjady, N., and Zareipour, H. "Multi-period stochastic security-constrained OPF considering the uncertainty sources of wind power, load demand and equipment unavailability", *Electr. Power Syst. Res.*, **146**, pp. 33-42 (2017).
20. Attarha, A., Amjady, N., and Conejo, A.J. "Adaptive robust AC optimal power flow considering load and wind power uncertainties", *Int. J. Electr. Power Energy Syst.*, **96**, pp. 132-142 (2018).
21. Wu, X., Conejo, A.J., and Amjady, N. "Robust security constrained ACOPF via conic programming: Identifying the worst contingencies", *IEEE Trans. Power Syst.*, **33**(6), pp. 5884-5891 (2018).
22. GAMS (2018): Generalized Algebraic Modelling System. [online], Available: http://www.gams.com. (n.d.).
23. Ahmadigorji, M. and Amjady, N. "A multiyear DG-incorporated framework for expansion planning of distribution networks using binary chaotic shark smell optimization algorithm", *Energy*, **102**, pp. 199-215 (2016).
24. Attarha, A. and Amjady, N. "Solution of security constrained optimal power flow for large-scale power systems by convex transformation techniques and Taylor series", *IET Gener. Transm. Distrib.*, **10**(4), pp. 889-896 (2016).
25. Wu, T., Zhang, Y.J., and Tang, X. "A VSC-based BESS model for multi-objective OPF using mixed integer SOCP", *IEEE Trans. Power Syst.*, **34**(4), pp. 2541-2552 (2019).
26. Erseghe, T. and Tomasin, S. "Power flow optimization for smart microgrids by SDP relaxation on linear networks", *IEEE Trans. Smart Grid*, **4**(2), pp. 751-762 (2013).
27. Bynum, M., Castillo, A., Watson, J.P., et al. "Tightening McCormick relaxations toward global solution of the ACOPF problem", *IEEE Trans. Power Syst.*, **34**(1), pp. 814-817 (2019).
28. Pareek, P. and Verma, A. "Linear OPF with linearization of quadratic branch flow limits", *2018 IEEMA Eng. Infin. Conf. ETechNxT 2018*, pp. 1-6 (2018).
29. Miao, Z., Fan, L., Aghamolki, H.G., et al. "Least squares estimation based SDP cuts for SOCP relaxation of AC OPF", *IEEE Trans. Automat. Contr.*, **63**(1), pp. 241-248 (2018).

Biographies

Mohammad Ali Tavakkoli received the BS and MS degrees in Electrical Engineering from Power and Water University of Technology, Iran, and Khajeh Nasir Toosi University of Technology, Iran, in 2003 and 2011, respectively. Currently, he is pursuing the PhD degree in Electrical Power Engineering in the Department of Electrical and Computer Engineering, Semnan University, Semnan, Iran. His doctoral studies focus on optimization problems in power systems, in particular, optimal power flow.

Nima Amjady received the BS, MS, and PhD degrees in Electrical engineering from Sharif University of Technology, Tehran, Iran, in 1992, 1994, and 1997, respectively. At present, he is a Full Professor at Semnan University, Semnan, Iran. He is also a consultant to Iran Grid Management Company. His research interests include application of machine learning and data mining in forecast processes of power systems as well as planning and operation of power systems.